An-Najah University Journal for Research – A
Natural Sciences

Preparation of Silver Nanoparticles/Polyvinyl alcohol Nanocomposite Films with Enhanced Electrical, Thermal, and Antimicrobial Properties

Shahd Salameh[1], Sondos Soboh[1], Abeer Bsharat[1], Raed Maali[2], Mohyeddin Assali[3], Maen Ishtaiwi[4], Muna Hajjyahya[4], Abdulraziq Zarour[5], Shadi Sawalha[1,*]
Received: 13th Dec. 2024, Accepted: 2th Feb. 2025, Published: ××××

Accepted Manuscript, In press

Abstract: Polyvinyl alcohol (PVA)/Silver (Ag) nanocomposites exhibit remarkable properties, including enhanced thermal, optical, electrical, and antibacterial characteristics. These properties are modulated by the preparation and addition of silver nanoparticles into polyvinyl alcohol films. The Ag-NPs were synthesized by a microwave-assisted method and, showed size-dependent properties, where the increase in microwave power resulted in increased nanoparticle sizes, reducing the energy bandgap from 2.93 eV to 2.55 eV. The electrical conductivity of the PVA film improved significantly from 0.065 S/m to 0.57 S/m, while its crystallinity increased from 14.047% to 18.331% with higher Ag-NP content. Additionally, UV-Vis absorption of the nanocomposite film increased with Ag-NP incorporation, reflecting uniform particle distribution. The antibacterial efficacy of these nanocomposites is particularly noteworthy. Smaller Ag-NPs, produced under lower microwave power, exhibited enhanced penetration through bacterial membranes, leading to improved antibacterial activity. This was evident in an 84% reduction of *E. coli* colony-forming units, from 36 to 6. The antibacterial activity against *E. Coli* bacteria makes the film highly suitable for various industrial applications. With their unique combination of electrical, thermal, and antibacterial properties, Ag/PVA nanocomposites hold significant promise for use in healthcare, packaging, and electronics.

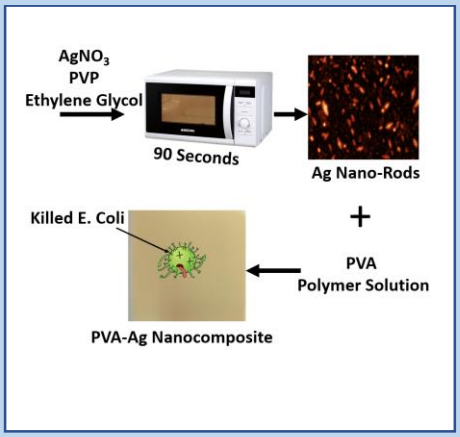

Keywords: Eco-Friendly Antibacterial Films (coatings), Biodegradable Packaging, Thermal Properties, Electrical Conductivity, Nanocomposites. Energy efficient Synthesis

Introduction

Silver nanoparticles (Ag-NPs), with their strong antibacterial qualities, have become a possible answer to the increasing problem of antibiotic resistance brought on by the common misuse of antibiotics (1). Ag-NPs are efficient against bacterial infections in a variety of medical applications, including stopping bacterial colonization on catheters, dental materials, and prosthesis (2). Recent developments in Ag-NP synthesis demonstrate this. The huge surface area and small size of Ag-NPs provide greater interaction with bacterial cells, releasing silver ions that cause bacterial cell death and disrupt essential biological functions (3). Notably, polyvinyl alcohol-based Ag-PVA nanoparticles stand out for their biocompatibility, stability, and effectiveness, making them suitable for wound dressings and medical treatments. Ag-PVA nanocomposites present an effective method to address the growing threat of bacterial resistance against traditional antibiotics by interacting with essential enzymes, breaking down bacterial membranes, and preventing the formation of biofilm (4).

Previous studies have extensively explored various methods for synthesizing PVA/Ag nanocomposites. For example, Chandran et al. employed a chemical reduction method to synthesize Ag nanoparticles within a PVA matrix, highlighting the enhanced antimicrobial properties of the composite (5). Similarly, Tavukcuogluet al. utilized a green synthesis approach by reducing Ag ions using plant extracts and successfully embedding the nanoparticles into a PVA matrix to develop biocompatible materials for medical applications (6). Furthermore, Iswarya et al. demonstrated the use of UV irradiation to reduce silver ions in a PVA solution, reporting a uniform dispersion of nanoparticles and significant improvements in the composite's mechanical and electrical properties (7)

1 Chemical Engineering Program, Faculty of Engineering and Information Technology, An-Najah National University, P.O.BOX 7 Nablus, Palestine
2 Department of Industrial Engineering, Al-Quds University, 20002 East Jerusalem, Palestine.
3 Department of Pharmacy, Faculty of Medicine and Health Sciences, An-Najah National University, P.O.BOX 7, Nablus, Palestine
4 Department of Physics, Faculty of Science, An-Najah National University, P.O.BOX 7, Nablus, Palestine.
5 5Department of Biomedical Sciences, Faculty of Medicine and Health Sciences, An-Najah National University, Nablus, P400, Palestine
*Corresponding author email: sh.sawalha@najah.edu

The synthesis of novel organic and inorganic nanocomposites, such as metal-polymer nanoparticles (5), is of great interest to material scientists. For example, silver (6), gold(Au), and iron(Fe) (7), nanoparticles are blended with a wide range of polymers to form nanocomposites with superior mechanical and physical properties (6). The combination of polyvinyl alcohol (PVA) with silver nanoparticles (Ag NPs) has attracted much interest (7). The resulting Ag/PVA nanocomposites show promise for various applications due to their unique properties (8) which include improved thermal stability, optical properties, electrical conductivity, and antimicrobial properties (9). PVA matrices incorporate silver, which has superior antibacterial characteristics, to optimize their synergistic effects. For the dispersion and immobilization of Ag NPs, PVA offers a flexible and reliable platform that provides enhanced mechanical, thermal, and biological properties (10). The resulting nanocomposites have enormous applications in industries including electronics, packaging, and medicine (11).

Silver nanoparticles (Ag NPs) have emerged as a subject of paramount interest within the realm of nanotechnology (12)owing to their unique properties and notable versatility across various applications. These nanoparticles are composed of silver atoms arranged on a nanoscale, typically between 1 and 100 nanometers(13).The diminutive size and consequential high surface area-to-volume ratio of Ag NPs contribute to their extraordinary physicochemical characteristics(14), including heightened catalytic, optical, and antimicrobial attributes(15).

Ag NPs can be synthesized through diverse methods(16), encompassing chemical reduction, physical techniques, and biological approaches(17). The applications of these nanoparticles span a wide array of fields, encompassing medicine, electronics, catalysis, and environmental remediation(18). Particularly noteworthy is their application in the medical domain, where their antimicrobial properties render them invaluable for various applications in wound healing, drug encapsulation, and biosensors (19).

This study focuses on the rapid synthesis of silver nanoparticles (Ag-NPs) utilizing a microwave-assisted approach, highlighting the unique role of microwave power in influencing their electrical and optical properties. Furthermore, the research aims to enhance the electrical, thermal, and antibacterial characteristics of polyvinyl alcohol (PVA) films. The novelty lies in leveraging microwave technology as an efficient and environmentally friendly method for synthesizing Ag-NPs, offering precise control over nanoparticle size and distribution while significantly reducing processing time compared to conventional techniques. This innovative approach also enables the development of multifunctional PVA films with improved performance for advanced applications.

Experimental Work

Materials: Silver Nitrate $AgNO_3$ (precursor), Ethylene glycol (reducing agent), Polyvinylpyrrolidone (PVP, MW = 40 kDa) as stabilizing agent, Polyvinyl alcohol (PVA, MW =30-70 kDa) (polymer), distilled water (solvent). All chemicals have been supplied by Sigma Aldrich and used without further purification.

Sample Preparation

Preparation of silver nanoparticles (Ag-NPs): 0.34 g of Polyvinylpyrrolidone (PVP) was dissolved in 40 ml Ethylene glycol at room temperature under continued stirring using a magnetic stirrer. When a homogeneous mixture was obtained, 0.17 g of $AgNO_3$ was added. The mixture consisting of $AgNO_3$ and PVP was heated by a domestic microwave at different powers medium-low (ML) (300- 400 W), medium (M) (400-500 W), medium-high (MH) (500-800 W), and high (H) (800- 1000 W) for 90 seconds.

Preparation of Polyvinyl alcohol (PVA) film and Ag nanocomposites: 1.0 g of PVA was dissolved in 50 ml of distilled water at 90°C under continued stirring using a magnetic stirrer. After the dissolving of PVA the Ag-NPs solution with a concentration of 2.23 mg/ml was added in different volumes (0.25 ml, 0.5 ml, 0.75 ml, 1.0 ml) to the PVA solution, as a result of this addition we get a different weight percent of Ag-NPs inside the PVA film. The homogeneous mixture was poured onto a clean, dry, leveled surface to obtain thin film nanocomposites. The film was left to dry naturally.

Sample Testing: UV–Vis absorption spectra for the Ag-NPs solution and PVA/Ag nanocomposite films were recorded using a Beckman Coulter DU 800 Spectrophotometer in the region of 300-600 nm. Gwydion software was used for the analysis of Atomic Force Microscopy (AFM) images. For AFM, a drop of a solution of Ag NPs was added onto mica substrates and was analyzed by coreAFM from Nanosurf company, Switzerland (20). The electrical conductivity of the prepared Ag NPs solution and PVA/Ag nanocomposite films was measured by a vector network analyzer (VNA). Thermal properties of the prepared samples were determined by using the Differential Scanning Calorimetry (DSC) model Pyrix-6, PerkinElmer Corporation, U.K. Each film sample (with Ag-NPs of 0, 0.11, and 0.22wt%) was heated from room temperature to 400°C at a rate of 10°C/min. The melting temperature and the heat of fusion were derived from the maximum peak and the area under the peak, respectively, which was essential for estimating the percentage of crystalline regions. The DSC test was performed following ASTM D3418-15 (21).

Antimicrobial Activity

Bacterial Strains: The study examined the antibacterial activity of Ag-NPs that were synthesized under ideal conditions adherence to CLSI/EUCAST guidelines, and proper biosafety practices (22). The strains of bacteria that were tested included: "*Escherichia coli* (ATCC 25922), *Staphylococcus aureus* (ATCC 25923*), methicillin-resistant Staphylococcus aureus* (MRSA) (DPC 5645), Klebsiella *pneumoniae* (ATCC 13883), *Proteus vulgaris* (ATCC 13315), and *Pseudomonas aeruginosa* (ATCC 27853)".

Preparation of the Bacterial Suspension: Three to four colonies were transferred under sterile conditions according to the CLSI standard to saline solution from a newly cultured plate containing bacteria in the log growth phase. The 0.5 McFarland reference solution was prepared by mixing 0.5 mL of 1.175% (w/v) $BaCl_2H_2O$ with 99.5 mL of 1% (v/v) H_2SO_4 and was used to correct the turbidity of the bacterial suspensions. When the turbidity reached 0.08−0.1, which corresponded to a bacterial concentration of 1.5 x 10^8 CFU/mL, the absorbance of the suspensions was read at λ = 630 nm using pure water as the reference blank. The McFarland solution was tightly wrapped in aluminum foil and sealed to prevent evaporation and to protect it from light (23).

Broth Microdilution Method:

The broth microdilution method was done in line with the CLSI protocol to determine the minimal inhibitory concentration (MIC) of synthesized Ag-NPs at different powers, L, LM, M, MH, and H. In each well of a 96-well plate, 100 µL of LB broth was added, then 100 µL of Ag-NPs synthesized at LM power (2.23 mg/mL) were added to the first well and serial dilutions by transferring 100 µL to the next wells, except wells 11 and 12. Then, 1 µL of bacterial suspension was added to each well except well 12 as the negative control. For all other sets of Ag-NPs synthesized at, the aforementioned steps were repeated. Then, the plates were incubated at 37°C overnight. MICs were determined

by observing the lowest concentration of each sample which prevents observable bacterial growth. (23).

Bacterial Growth Reduction (CFU): Three flasks were prepared and added with 90 mL of sterilized water in each. Then, 10 mL of E. coli solution was added to each flask. Ag/PVA film was introduced to one of the flasks, while pure PVA film was added into another. The third flask acted as a blank control. Further dilution of each material to 1x10^5 of the original concentration followed after one hour's stir of all three flasks using an orbital shaker. From each of these dilutions, 1 mL was seeded into a Petri dish to which Luria-Bertani agar was added. All the plates then were incubated at 37 °C for 12 h. The surviving numbers of E. coli were enumerated by counting bacterial colonies (24).

Results and Discussion

Synthesis of Ag-NPs

Ag-NPs were prepared using $AgNO_3$ as a precursor and ethylene glycol as a reducing agent while polyvinyl pyrrolidone as a stabilizing agent. Silver nitrate will be used to provide the required ions of silver that will be reduced to Ag^0. Ethylene glycol plays an important role in the reduction of silver ions into silver nanoparticles was achieved utilizing ethylene glycol. The high viscosity of PVP plays an important role in stabilizing the colloid viscosity and also controls the reduction rate, which impacts the size and shape of nanoparticles, preventing nanoparticle aggregation. Under microwave irradiation, the reducing agent initiates the reduction of silver ions to form nucleation sites, these nucleation sites then act as seeds for the growth of silver nanoparticles (25). The microwave power accelerates the reaction kinetics by rapidly heating the reaction mixture(26). This accelerated the time needed within the 90s and gave a product yield of 22.11%.

Optical properties

The optical characteristics of the prepared Ag-NPs and PVA/Ag nanocomposite films were determined by UV-Vis. Fig.1(a) illustrates the UV-Vis absorption spectra for the prepared Ag-NPs at various powers. The surface plasmon resonance band at 450 nm was observed for all powers except for 400 nm for M-L power. With an increase in power, the plasmon peak shifts to a longer wavelength and becomes wider, indicating that power affects the size, as the size increases, this shift occurs and the peak becomes wider (25). Furthermore, the energy band gap was determined by applying the Tauc equation and drawing the Tauc plot (27), the Tauc equations:

$$(\alpha h\upsilon)^n = B(h\nu - E) \quad (1)$$

$$(\alpha h\upsilon)^{1/n} = B(h\nu - E) \quad (2)$$

where α is the absorbance coefficient, n is a factor that depends on the electron transition property, B is a constant, h is the Plank constant, υ is the photon frequency, and E is the band gap energy. for a direct band gap (n = ½) and an indirect band gap (n = 2) as shown in Fig.2 Considering the direct band gap, Plotting the values of $(\alpha h\nu)^2$ against $h\nu$ and extrapolating along the linear region along the X-axis on the energy bandgap in electron volts, an estimate of the energy gap. as shown in Fig.1 Considering the indirect band gap as in Fig. 1, we noticed that increasing the power led to a decrease in the band gap from 2.93 eV to 2.55eV. This decrease in the band gap could be due to increased size with increasing power.

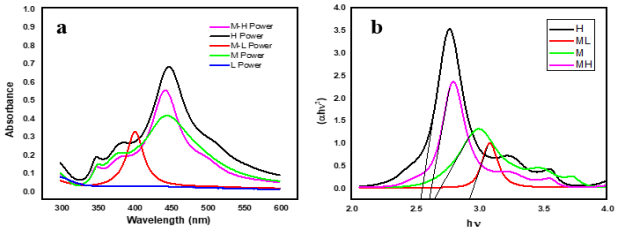

Figure 1:(a) UV-vis absorption spectra of synthesized Ag-NPs at different power, (b) Tauc plot of Ag-NPs at different power.

Furthermore, the UV-Vis absorption was examined for the prepared PVA/Ag nanocomposite films as shown in Fig.2(a). By increasing the amount of Ag-NPs in the PVA film, there is a clear increase in its absorption. Also, we noticed the presence of plasmonic peaks, and this is evidence of the presence of Ag-NPs particles in the film, as it increases, the intensity increases and the absorption becomes higher. On the other hand, there is a slight effect of the concentration on the band gap as explained in Fig.2, because the Ag-NPs solution is synthesized at the same power, so the size stays the same. The slight change in the band gap is the result of the distribution of Ag-NPs within the film.

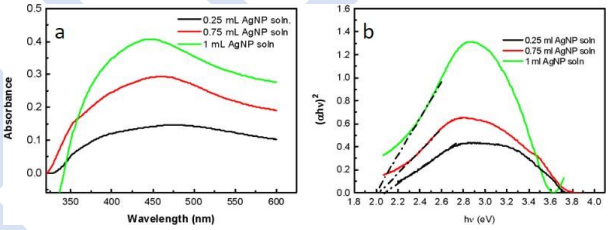

Figure 2:(a) UV-vis absorption spectra of prepared PVA / Ag nanocomposite Tauc plot of PVA / Ag nanocomposite at medium-high power.

Electrical properties

The electrical conductivity of Ag NPs solutions synthesized using different powers is given in Fig.3(a), as the power increases the electrical conductivity increases, this was due to the rise in the size with power and the decrease in band gap(28). Moreover, the electrical conductivity of PVA film increases with the amount of Ag-NPs added to the film. In Fig. 3, we noticed an increase in the conductivity of PVA film with 0.0 ml of Ag-NPs (pure PVA) from 0.065 s/m to 0.570 s/m for PVA film with 1 ml of Ag-NPs solution.

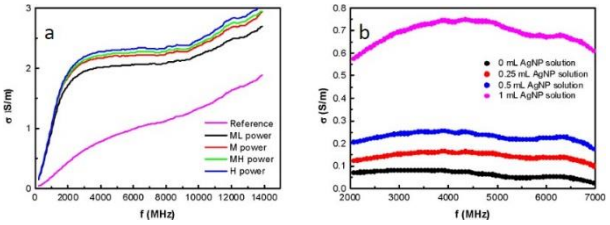

Figure 3: (a) the electrical conductivity of synthesized Ag-NPs, and (b) the electrical conductivity of synthesized PVA / Ag nanocomposite with different volume Ag-NPs.

Atomic Force Microscopy (AFM)

AFM was used to study the morphology and size of formed Ag-NPs. It's clear from Fig.4 that the formed Ag-NPs are rod-like nanomaterial affected by the power. The Ag-NPs exhibit a rod-like nanomaterial structure, and their size varies depending on the power applied. In the case of medium power, we observed rods with diameters ranging from approximately 5 nm to 20 nm.

ACCEPTED

Furthermore, the obtained Ag nanorods exhibit sizes ranging from 20 nm to 80 nm for high- medium power.

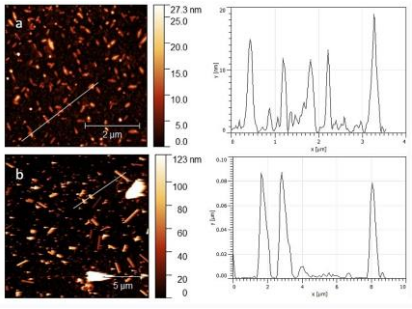

Figure 4:(a) The morphology and size for Ag-NPs at medium power, (b) The morphology and size for Ag-NPs at medium-high power.

Differential Scanning Calorimetry (DSC)

Based on the Differential Scanning Calorimetry (DSC) analysis, the effects of adding 0.0 wt%, 0.11wt%, and 0.22wt% of Ag-NPs (silver nanoparticles) to PVA on its heat flow as a function of temperature were investigated. DSC curves (Fig.5) show distinct peaks, indicating different thermal transitions occurring within the samples.

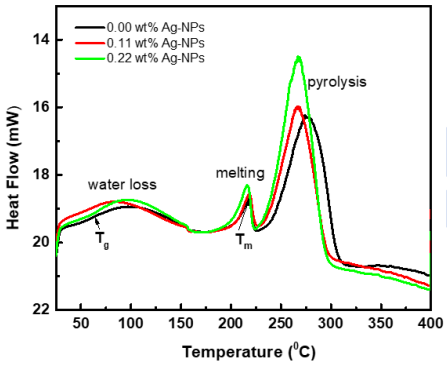

Figure 5: DSC results for Ag/PVA nanocomposite film containing different wt% of Ag-NPs.

The results demonstrate that as the content of Ag-NPs increases, there is a noticeable shift in the thermal behavior of PVA. Specifically, the introduction of Ag-NPs causes a slight decrease in the melting point of PVA, depending on the Ag-NPs. The results are summarized in Table 1.

Table 1: DSC results for Melting Enthalpy (ΔHm), Melting Peak Temperature (*Tm*), and Glass Transition Temperatures (*Tg*) of PVA and PVA/Ag Nanocomposites, %Degree of crystallinity.

Wt% Ag	Tg	Tm	ΔHm/J g^{-1}	Xc %
0.0 Pure PVA	83.87	218.62	-19.38	14.05
0.11 Ag-NPs	80.10	218.28	-19.71	14.20
0.22 Ag-NPs	78.89	216.48	-21.47	18.33

Crystallinity also changed with the addition of Ag-NPs. The percentage of crystalline regions can be calculated using the formula(29):

$$Xc = \frac{\Delta H_f}{\Delta H^\circ_f \times \mathrm{X}} \times 100\%$$

Where Xc is the percent of crystalline regions, H_f is the heat of fusion of the sample; $\Delta \boldsymbol{H}^\circ_f$ is the heat of fusion for 100% crystalline PVA which is found to be 138J/g, and *X* is the weight percent of polymer (PVA) in the produced composite. The results show the sample containing 0.22 wt% Ag-NPs exhibits the highest percentage of crystallinity compared to other tested samples. The slight increase in crystallinity is attributed to the nucleating effect of Ag-NPs, which promotes the formation of more ordered crystalline regions within the PVA matrix (30).

Additionally, the increased mobility of polymer chains near the Ag-NPs may contribute to a significant decrease in the glass transition temperature for the nanocomposite containing 0.22 wt% of Ag-NPs which act as plasticizers (31).

Antibacterial Activity

The minimum inhibitory concentration (MIC) of Ag-NPs synthesized at different powers (L, ML, M, MH, H) was determined using the broth microdilution method against different bacterial strains and reported quantitatively in Table 2.

Table 2: MIC values (µg/mL) of different powers for the Microbial and Fungal Growth Inhibition.

ATCC Number	microbe Strain	Gram type	Power				
			L	ML	M	MH	H
DPC 5645	MRSA	+ ve	20	17	18	183	330
ATCC 25923	S. aureus	+ ve	20	17	18	183	330
ATCC 25922	E. coli	- ve	10	8.6	18	91	330
ATCC 13883	Klebsiella pneumoniae	- ve	5	4.3	4.6	45	330
ATCC 8427	Proteus vulgaris	- ve	20	8.6	18	45	160
ATCC 9027	Pseudomonas aeruginosa	- ve	5	4.3	4.6	45	330

Furthermore a decrease in MIC with lower power could be related to smaller Ag-NPS with an ability to penetrate the cell membrane easily compared to large ones which improve their antibacterial activity (32).

Moreover, the Ag/PVA nanocomposite film containing 0.22% Ag particles caused a colony forming units' reduction from 36 to 6 with a reduction percent of 84% for the *E. coli* bacteria.

Conclusion

In this work, Ag-NPs solution was prepared from $AgNO_3$ using PVP as a stabilizing agent, and Ethelyn glycol as a reducing agent at different power levels using the microwave chemical reduction method. As the power increased, the particle size increased, and the band gap decreased. Different Ag-NPs prepared at medium-low power were combined with PVA polymer to give Ag/PVA nanocomposite film. The absorption of Ag/PVA nanocomposite film increases with increasing Ag-NP concentration and has a slight effect on the band gap, the slight difference in the band gap resulting from the distribution of the particles within the PVA film, the degree of crystallinity of PVA film increases with increasing the wt% of Ag-NPs added to the film, The decrease in power lead to a decrease in the Ag-NPs' size, inducing an increase in their ability to penetrate the cell membrane, improving antibacterial activity for Ag-NPs. Ag/PVA nanocomposite film caused high colony-forming unit reduction, for the *E. coli* bacteria.

ACCEPTED

Author's contribution: The authors confirm the contribution to the paper as follows: study conception and design: Sawalha Sh., Salameh Sh., Soboh S., and Bsharat A., theoretical calculations and modeling: Sawalha Sh., Salameh Sh., Soboh S., and Bsharat A, data analysis, and validation: Sawalha Sh., Assali M., Maali R., Ishtaiwi M., Abdulraziq Zarour and Hajjyahya Muna, draft manuscript preparation: Salameh Sh., Supervision: Sawalha Shadi

Ethics approval and consent to participate:

Not applicable

Consent for publication:

Not applicable

Availability of data and materials: The raw data required to reproduce these findings are available in the body and illustrations of this manuscript.

Funding:

No funding is available

Conflicts of interest:

The author declares that there is no conflict of interest regarding the publication of this article

Acknowledgment: The authors would like to acknowledge An-Najah National University (www.najah.edu) for its support.

References

1. Ismail H, Zaaba N. Effect of additives on properties of polyvinyl alcohol (PVA)/tapioca starch biodegradable films. Polymer-Plastics Technology and Engineering. 2011;50(12):1214-9.
2. Franci G, Falanga A, Galdiero S, Palomba L, Rai M, Morelli G, et al. Silver nanoparticles as potential antibacterial agents. Molecules. 2015;20(5):8856-74.
3. Chapa C. Bactericidal activity of silver nanoparticles in drug-resistant bacteria. Instituto de Ingeniería y Tecnología. 2023.
4. Bruna T, Maldonado-Bravo F, Jara P, Caro N. Silver nanoparticles and their antibacterial applications. International journal of molecular sciences. 2021;22(13):7202.
5. Yan Y, Yang G, Xu J-L, Zhang M, Kuo C-C, Wang S-D. Conducting polymer-inorganic nanocomposite-based gas sensors: a review. Science and Technology of Advanced Materials. 2020;21(1):768-86.
6. Lyapina M, Cekova M, Krasteva A, Dencheva M, Yaneva-Deliverska M, Kisselova A. Physical properties of nanocomposites in relation to their advantages. Journal of IMAB–Annual Proceeding Scientific Papers. 2016;22(1):1056-62.
7. Mostafa AM, Menazea A. Polyvinyl Alcohol/Silver nanoparticles film prepared via pulsed laser ablation: An eco-friendly nano-catalyst for 4-nitrophenol degradation. Journal of Molecular Structure. 2020;1212:128125.
8. Palanichamy K, Anandan M, Sridhar J, Natarajan V, Dhandapani A. PVA and PMMA nano-composites: a review on strategies, applications and future prospects. Materials Research Express. 2023;10(2):022002.
9. Koduru H, Marino L, Janardhanam V, Scaramuzza N. Influence of thin layer of silver nanoparticles on optical and dielectric properties of poly (vinyl alcohol) composite films. Surfaces and Interfaces. 2016;5:47-54.
10. Mejía ML, Moncada ME, Ossa-Orozco CP, editors. Poly (vinyl alcohol)/Silk Fibroin/Ag NPs composite nanofibers for bone tissue engineering. 2021 43rd Annual International Conference of the IEEE Engineering in Medicine & Biology Society (EMBC); 2021: IEEE.
11. Rao MM, Mohammad N, Banerjee S, Khanna PK. Synthesis and Food Packaging Application of Silver Nano-Particles: A Review. Hybrid Advances. 2024:100230.
12. Mateo EM, Jiménez M. Silver nanoparticle-based therapy: can it be useful to combat multi-drug resistant bacteria? Antibiotics. 2022;11(9):1205.
13. Mukherji S, Bharti S, Shukla G, Mukherji S. Synthesis and characterization of size-and shape-controlled silver nanoparticles. Physical Sciences Reviews. 2019;4(1):20170082.
14. Nikzamir M, Akbarzadeh A, Panahi Y. An overview on nanoparticles used in biomedicine and their cytotoxicity. Journal of Drug Delivery Science and Technology. 2021;61:102316.
15. Limpan N, Prodpran T, Benjakul S, Prasarpran S, editors. Influences of degree of hydrolysis and molecular weight of poly (vinyl alcohol)(PVA) on properties of biodegradable films based on fish myofibrillar protein and PVA blend. 47 Kasetsart University Annual Conference, Bangkok (Thailand), 17-20 Mar 2009; 2009.
16. Yaqoob AA, Umar K, Ibrahim MNM. Silver nanoparticles: various methods of synthesis, size affecting factors and their potential applications–a review. Applied Nanoscience. 2020;10(5):1369-78.
17. Xu L, Wang Y-Y, Huang J, Chen C-Y, Wang Z-X, Xie H. Silver nanoparticles: Synthesis, medical applications and biosafety. Theranostics. 2020;10(20):8996.
18. Javed R, Zia M, Naz S, Aisida SO, Ain Nu, Ao Q. Role of capping agents in the application of nanoparticles in biomedicine and environmental remediation: recent trends and future prospects. Journal of Nanobiotechnology. 2020;18:1-15.
19. Liu B, Zhang J, Guo H. Research progress of polyvinyl alcohol water-resistant film materials. Membranes. 2022;12(3):347.
20. Hamed R, Sawalha S, Assali M, Shqair RA, Al-Qadi A, Hussein A, et al. Visible light-driven ZnO nanoparticles/carbon nanodots hybrid for broad-spectrum antimicrobial activity. Surfaces and Interfaces. 2023;38.
21. Jaques NG, Silva IDdS, Barbosa Neto MdC, Ries A, Canedo EL, Wellen RMR. Effect of heat cycling on melting and crystallization of PHB/TiO2 compounds. Polímeros. 2018;28(2):161-8.
22. Gajic I, Kabic J, Kekic D, Jovicevic M, Milenkovic M, Mitic Culafic D, et al. Antimicrobial Susceptibility Testing: A Comprehensive Review of Currently Used Methods. Antibiotics (Basel). 2022;11(4).
23. Sawalha S, Assali M, Raddad M, Ghneem T, Sawalhi T, Almasri M, et al. Broad-Spectrum Antibacterial Activity of Synthesized Carbon Nanodots from d-Glucose. ACS Applied Bio Materials. 2022;5(10):4860-72.
24. Ruiz S, Tamayo JA, Delgado Ospina J, Navia Porras DP, Valencia Zapata ME, Mina Hernandez JH, et al. Antimicrobial Films Based on Nanocomposites of Chitosan/Poly(vinyl alcohol)/Graphene Oxide for Biomedical Applications. Biomolecules. 2019;9(3).
25. Makuła P, Pacia M, Macyk W. How to correctly determine the band gap energy of modified semiconductor photocatalysts based on UV–Vis spectra. ACS Publications; 2018. p. 6814-7.
26. Xie H-F, Yu C-J, Huang Y-L, Xu H, Zhang Q-L, Sun X-H, et al. 7RX, UK.† Footnotes relating to the title and/or authors should appear here. Electronic Supplementary Information (ESI) available: 1H/13C NMR spectra and the absorption spectra of probe, etc. See DOI: 10.1039/x0xx00000x. School of Public Health, the key Laboratory of Environmental Pollution Monitoring and Disease Control.
27. Klein J, Kampermann L, Mockenhaupt B, Behrens M, Strunk J, Bacher G. Limitations of the Tauc plot method. Advanced Functional Materials. 2023;33(47):2304523.
28. Yakuphanoglu F, Şenkal BF, Saraç A. Electrical conductivity, thermoelectric power, and optical properties of organo-soluble polyaniline organic semiconductor. Journal of Electronic Materials. 2008;37:930-4.
29. Sawalha S, Ma'ali R, Surkhi O, Sawalha M, Dardouk B, Walwel H, et al. Reinforcing of low-density polyethylene by cellulose extracted from agricultural wastes. Journal of Composite Materials. 2019;53(2):219-25.

30. Ming Y, Zhou Z, Hao T, Nie Y. Polymer Nanocomposites: Role of modified filler content and interfacial interaction on crystallization. European Polymer Journal. 2022;162.
31. Pandis C, Logakis E, Kyritsis A, Pissis P, Vodnik VV, Džunuzović E, et al. Glass transition and polymer dynamics in silver/poly(methyl methacrylate) nanocomposites. European Polymer Journal. 2011;47(8):1514-25.
32. Herman A, Herman AP. Nanoparticles as antimicrobial agents: their toxicity and mechanisms of action. Journal of Nanoscience and Nanotechnology. 2014;14(1):946-57.

ACCEPTED